BBA - Molecular Basis of Disease 1866 (2020) 165922

Contents lists available at ScienceDirect

BBA - Molecular Basis of Disease

journal homepage: www.elsevier.com/locate/bbadis

I-152, a supplier of *N*-acetyl-cysteine and cysteamine, inhibits immunoglobulin secretion and plasma cell maturation in LP-BM5 murine leukemia retrovirus-infected mice by affecting the unfolded protein response

Alessandra Fraternale[a,*], Carolina Zara[a], Tomas Di Mambro[a], Elisabetta Manuali[b], Domenica Anna Genovese[b], Luca Galluzzi[a], Aurora Diotallevi[a], Andrea Pompa[a], Francesca De Marchis[c], Patrizia Ambrogini[a], Erica Cesarini[a], Francesca Luchetti[a], Michaël Smietana[d], Kathy Green[e], Francesca Bartoccini[a], Mauro Magnani[a], Rita Crinelli[a]

[a] *Department of Biomolecular Sciences, University of Urbino Carlo Bo, Via Saffi 2, 61029 Urbino, Italy*
[b] *Laboratory of Histopathology and Clinical Chemistry, Istituto Zooprofilattico Sperimentale dell'Umbria e delle Marche "Togo Rosati", 06126 Perugia, Italy*
[c] *CNR, Institute of Biosciences and Bioresources (IBBR), 06128 Perugia, Italy*
[d] *Institut des Biomolécules Max Mousseron, Université de Montpellier UMR 5247 CNRS, ENSCM, 34095 Montpellier, France*
[e] *Department of Microbiology and Immunology, Geisel School of Medicine at Dartmouth, Lebanon, NH 03766, USA*

ARTICLE INFO

Keywords:
Hypergammaglobulinemia
UPR
Endoplasmic reticulum
Glutathione pro-drug
Murine AIDS

ABSTRACT

Excessive production of immunoglobulins (Ig) causes endoplasmic reticulum (ER) stress and triggers the unfolded protein response (UPR). Hypergammaglobulinemia and lymphadenopathy are hallmarks of murine AIDS that develops in mice infected with the LP-BM5 murine leukemia retrovirus complex. In these mice, Th2 polarization and aberrant humoral response have been previously correlated to altered intracellular redox homeostasis. Our goal was to understand the role of the cell's redox state in Ig secretion and plasma cell (PC) maturation. To this aim, LP-BM5-infected mice were treated with I-152, an *N*-acetyl-cysteine and cysteamine supplier. Intraperitoneal I-152 administration (30 μmol/mouse three times a week for 9 weeks) decreased plasma IgG and increased IgG/Syndecan 1 ratio in the lymph nodes where IgG were in part accumulated within the ER. PC containing cytoplasmic inclusions filled with IgG were present in all animals, with fewer mature PC in those treated with I-152. Infection induced up-regulation of signaling molecules involved in the UPR, i.e. CHAC1, BiP, sXBP-1 and PDI, that were generally unaffected by I-152 treatment except for PDI and sXBP-1, which have a key role in protein folding and PC maturation, respectively. Our data suggest that one of the mechanisms through which I-152 can limit hypergammaglobulinemia in LP-BM5-infected mice is by influencing IgG folding/assembly as well as secretion and affecting PC maturation.

1. Introduction

A syndrome characterized by lymphadenopathy, hypergammaglobulinemia, and immunodeficiency, known as murine AIDS (MAIDS), develops in C57BL/6 mice infected with LP-BM5 murine leukemia viruses [1–4]. Several abnormalities in immune function are characteristic of mice with MAIDS [5–7]. An early period characterized by high viral replication and immune responsiveness is followed by a lasting and profound immunosuppression that affects several aspects of cellular and humoral immunity [4]. LP-BM5 infection induces progressive lymph proliferation and most lymphoid cells are involved in the proliferative process [4]. Alterations in the humoral immune system such as rapid B cell proliferation, polyclonal activation of B cells, increase in Ig-secreting B cells and development of significant hypergammaglobulinemia have been described [4,8].

The terminal differentiation of B cells to plasma cells (PC) requires

Abbreviations: ABTS, 2,2′-azino-di-(3-ethylbenzothiazoline)-6-sulfonic acid); ATF6, activating transcription factor 6α (ATF6α); BiP, binding immunoglobulin protein; CHAC1, ChaC glutathione-specific γ-glutamylcyclotransferase 1; ER, endoplasmic reticulum; GSH, reduced glutathione; HRP, horseradish peroxidase; IgG, immunoglobulins G; IRE1, inositol-requiring transmembrane kinase/endonuclease 1; MAIDS, murine AIDS; PC, plasma cell; PDI, protein disulfide isomerase; PERK, PKR-like endoplasmic reticulum kinase (PERK); s-XBP-1, spliced X-box-binding protein 1; UPR, unfolded protein response

* Corresponding author at: Department of Biomolecular Sciences, University of Urbino Carlo Bo, 61029 Urbino, Italy.
E-mail address: alessandra.fraternale@uniurb.it (A. Fraternale).

https://doi.org/10.1016/j.bbadis.2020.165922
Received 14 April 2020; Received in revised form 16 July 2020; Accepted 8 August 2020
Available online 12 August 2020
0925-4439/

important changes in both the cellular structure and function [9]. During PC differentiation, the production of Ig heavy and light chain transcripts and proteins are significantly elevated. This coincides with a significant expansion of the rough endoplasmic reticulum (ER) where the nascent Ig chains are folded, assembled and, inspected by the ER quality control apparatus [10]. Moreover, in a viral infection, viruses exploit cellular machineries and resources to complete their life cycle. In virus-infected cells, the cellular translation machinery is hijacked by the infecting virus to produce large amounts of viral proteins, which inevitably perturb ER homeostasis and cause ER stress [11]. Disturbances of ER homeostasis cause overload of unfolded or misfolded proteins in the ER lumen resulting in ER stress with subsequent triggering of cytoprotective signaling pathway (UPR). ER stress can activate three parallel pathways: PKR-like endoplasmic reticulum kinase (PERK), activating transcription factor 6α (ATF6α), and inositol-requiring transmembrane kinase/endonuclease 1 (IRE1) [12].

The UPR up-regulates synthesis of ER chaperones and folding enzymes, i.e. BiP (Binding immunoglobulin protein), also referred to as Hspa5 (Heat shock 70-kDa protein 5) or GRP78 (glucose-regulated protein 78), protein disulfide isomerase (PDI), and transcription factors, i.e. X-box binding protein 1 (XBP-1) to ensure efficient antibody (Ab) assembly and to coordinate the enhanced membrane biosynthesis necessary for generation of the highly developed ER network that is characteristic of PC [9,13–15]. Hence, UPR signaling has increasingly been shown to have a crucial role in immunity [16]. Of the three ER stress responses, the best studied in PC is the IRE1 pathway. IRE1 is an ER-localized transmembrane protein with endoribonuclease activity that excises a 26-nt sequence from XBP-1 messenger RNA (mRNA) [17,18]. This event, termed XBP-1 splicing, shifts the reading frame to excise a premature stop codon, resulting in a full-length functional XBP-1 protein product (sXBP-1). sXBP-1 then translocates to the nucleus where it induces target genes expression involved in protein synthesis and secretion [19–21]. XBP-1 expression is induced dramatically during PC differentiation in response to cytokines such as IL-4 and it is required for high Ig expression and the morphological changes that enable the PC to secrete large amounts of Ab [22–24]. Recent studies support the view that ER protein folding pathways are highly correlated with ROS production and that redox homeostasis is crucial for correct protein folding process and disulfide bond formation [25–27]. Moreover, the correct concentrations of glutathione are necessary to maintain ER oxidoreductases in a reduced form or facilitate the reduction of polypeptides destined for retro-translocation from the ER to the cytosol for degradation [28].

We have previously demonstrated that LP-BM5 infection induces significant drops in reduced glutathione (GSH) and/or cysteine concentration early during infection, i.e. 2–5 weeks post infection (p.i.), when the viral replicative rate is high and a Th2-type cytokine polarization develops [5]. Moreover, the treatment of LP-BM5-infected mice with a pro-GSH molecule [*N*-(*N*-acetyl-L-cysteinyl)-*S*-acetylcysteamine] named I-152, increases GSH levels in several organs and shifts the immune response towards the cellular immunity by influencing early Th1/Th2 cytokine secretion [5,29]. In this study, we investigated whether I-152 treatment could also affect the later phase of the disease characterized by the lymphoproliferative process and high IgG production. We found that the infection induced the major UPR components and increased the expression of UPR targets including the ER chaperons. I-152 treatment lowered plasma IgG concentration and partially accumulated IgG inside the ER of PC. In the lymph nodes of infected/treated mice, fewer mature PC and a decrease in PDI and sXBP-1 expression were found. Taken together, these results suggest that I-152 treatment inhibits total IgG production by interfering with maturation and secreting capacity of PC as well as with the folding of Ig.

2. Materials and methods

2.1. Ethics statement

Adult mice were used according to the Italian law on animal experimentation (D.lgs 26/2014; research project permitted with authorization N. 279/2015-PR by Italian Ministry of Health). Every effort was made to minimize the number of animals used and their suffering.

2.2. Mice

Four-week-old female C57BL/6 (B6) mice were purchased from Charles River Laboratories Italy and housed in the animal facility of the Department of Biomolecular Sciences (University of Urbino), which is approved by the Health Ministry of Italy.

2.3. LP-BM5 virus inoculation and treatment with I-152

The LP-BM5 viral mixture was prepared by co-culturing G6 cells with uninfected SC-1 cells as previously described [2]. C57BL/6 mice were infected by two successive intraperitoneal (i.p.) injections at 24-h intervals of the LP-MB5 murine leukemia virus stock, in which each injection contained 0.25 units of reverse transcriptase. A group of LP-BM5-infected mice was left untreated (infected mice, I); another one was treated with i.p. injections of I-152 (30 μmol/mouse) three times a week, every other day, for a total of 9 weeks (infected/treated mice, I + I-152). I-152 was synthesized as previously described [30]. Mice were sacrificed at specific time points: early in the course of infection, i.e. 2 weeks post infection (p.i.), when a severe immunological reaction in response to infection develops; 5 weeks, when B cell proliferation and increased number of Ig-secreting cells result in the development of hypergammaglobulinemia and enlarged lymphoid organs; 9 weeks, when the absolute number of Ig-secreting cells and circulating Ig levels do not change or decline.

2.4. Plasma IgG, IgG1 and IgG2a determination

Total IgG, IgG1 and IgG2a levels were determined using an enzyme-linked immunosorbent assay (ELISA) technique as previously described [31]. Briefly, the microplates (Nunc-immuno Plate MaxiSorp Surface, Nunc) were coated with goat anti-mouse IgG (Sigma-Aldrich, Milan, Italy), IgG1 or IgG2a (Bio-Rad, Hercules, CA, USA). After blocking with 5% bovine serum albumin (BSA), serial dilutions of murine plasma were added to each well. Immunocomplexes were revealed by using goat anti-mouse IgG-horseradish peroxidase (HRP) conjugated (Bio-Rad, Richmond, CA, USA), and the 2,2′-azino-di-(3-ethylbenzthiazoline sulfonic acid) or ABTS (Roche Diagnostic, Penzberg, Germany) substrate. Absorbance was measured at 405 nm on a Model Benchmark Microplate reader (Bio-Rad, Hercules, CA, USA). Absolute plasma IgG concentrations were calculated using known concentrations of standard mouse IgG.

2.5. Gene expression analysis

Total RNA was extracted with miRNeasy mini kit (Qiagen) from lymph nodes (7–20 mg) disrupted in 700 μL Qiazol and homogenized using QIAshredder spin columns (Qiagen, Hilden, Germany). The cDNA was synthesized using the PrimeScript™ RT Master Mix (Perfect Real Time) (Takara, Kusatsu, Shiga, Japan) from 0.5 μg total RNA, according to the manufacturer's instructions.

The real time PCR reactions were performed in a RotorGene 6000 instrument (Corbett life science, Sydney, Australia) in duplicate, using RT^2 SYBR® Green ROX FAST Mastermix (Qiagen, Hilden, Germany) and the primers listed in Table 1. The amplification conditions were: 95 °C for 10 min, 40 cycles at 95 °C for 10 s and 60 °C for 50 s. Relative mRNA expression was determined with the $2^{-\Delta\Delta Ct}$ method [32,33], using β-2

Table 1
Target mRNA and real time PCR primers used in this study.

mRNA	Accession number	Primer F (5′-3′)	Primer R (5′-3′)	Ref
B2M	NM_009735	TGCTATCCAGAAAACCCCTCAA	GGATTTCAATGTGAGGCGGG	[32]
BiP	NM_001163434	TCCGGCGTGAGGTAGAAAAG	GGCTTCATGGTAGAGCGGAA	[32]
CHAC1	NM_026929	TATAGTGACAGCCGTGTGGG	GCTCCCCTCGAACTTGGTAT	[32]
sXBP-1	NM_001271730	CTGAGTCCGCAGCAGGT	TGTCCAGAATGCCCAAAAGG	[32]
P4hb (PDI)	NM_011032	GATCAAGCCCCACCTGATGA	ACCTCTTCAAAGTTCGCCCC	[33]

B2M, *Mus musculus* Beta-2-Microglobulin; BiP, *Mus musculus* heat shock protein 5; CHAC1, *Mus musculus* ChaC, cation transport regulator 1; sXBP-1, *Mus musculus* X-Box Binding Protein 1, transcript variant 2 (spliced); P4hb (PDI), *Mus musculus* prolyl 4-hydroxylase, beta polypeptide (Protein disulfide-isomerase).

microglobulin (B2M) as a reference gene and uninfected mice as calibrator.

2.6. Organ homogenization and western immunoblotting analysis

The lymph nodes were excised flash frozen in dry ice and stored at −80 °C until processing. Organs were homogenized by sonication at 100 W in 8 volumes (w/v) of a buffer containing 50 mM Tris-HCl, pH 7.8, 0.25 M sucrose, 2% (w/v) SDS (Sodium Dodecyl Sulphate), 10 mM N-ethylmaleimide, completed with a cocktail of protease (Roche, Basilea, Switzerland) and phosphatase inhibitors (1 mM NaF, 1 mM Na_3VO_4). The lysates were boiled and, after centrifugation, the protein content was determined in the supernatant by the Lowry assay, using bovine albumin as a standard. Proteins were resolved by SDS-PAGE and electroblotted onto a PVDF membrane (0.2 μm) (Bio-Rad, Hercules, CA, USA). The blots were probed with the following primary antibodies: anti-BiP (C05B12) and anti-PDI (C81H6) from Cell Signaling Technology (Danvers, Massachusetts, USA); anti-XBP-1 (M-186, sc-7160) and anti Syndecan-1 (H-174, sc-5632) from Santa Cruz Biotechnology Inc. (Dallas, Texas, USA). Anti-Actin (A 2066, Sigma-Aldrich, Milan, Italy) was used to check equal protein loading. The bands were detected by HRP-conjugate secondary antibody (Bio-Rad, Hercules, CA, USA) and the HRP activity was detected with the enhanced chemiluminescence detection kit WesternBright ECL (Advansta, Bering Dr., San Jose, CA USA). Lymph node IgG levels were detected by using goat anti-mouse IgG (H + L) HRP-conjugate (Bio-Rad, Hercules, CA, USA). Immunoreactive bands were visualized in a ChemiDoc MP Imaging System and quantified with the Image Lab software (Bio-Rad, Hercules, CA, USA) with local background subtraction. Target protein intensity values were normalized on actin and the ratio reported in the graphs as arbitrary units.

2.7. Subcellular fractionation

IgG subcellular localization was studied by fractionation of lymph node homogenates by differential centrifugation. The lymph nodes were homogenized in a buffer consisting of 12% (w/v) sucrose, 10 mM KCl, 2 mM $MgCl_2$, 100 mM Tris-HCl, pH 7.8. A continuous gradient between 16% and 55% (w/v) sucrose was made using the same buffer, and 1 mL of the homogenate was loaded on top of the gradient. After centrifugation at 141,000 ×*g* for 4 h at 4 °C in a Beckman SW28 rotor, fractions of 0.780 mL were collected. An equal aliquot of each fraction was analyzed by SDS-PAGE and protein blot with anti-mouse IgG-HRP and anti-BiP antibodies (as above).

2.8. Histological analysis

The lymph nodes were fixed in 10% neutral buffered formalin and paraffin-embedded with standard procedures. Four μm thick sections were stained with Hematoxylin and Eosin (H&E) for histological and morphological investigations. Image digitization and semiquantitative analysis of PC were performed using the microscope Eclipse Ci-L (Nikon Corporation, Japan) and NIS-Elements Br-2 as software (v 5.10; Nikon). For semiquantitative analysis, the sections were initially scanned at intermediate (20×) magnification to assess the distribution of PC. Then, at high magnification (40×), the fields containing more PC, were analyzed and the average of the counts of the cells performed in 5 microscopic fields was calculated.

Among the PC observed, a discrimination between mature (differentiated) and immature (undifferentiated) PC, was performed. Differentiated PC have a heavily clumped chromatin network, absence of nucleolus, a perinuclear pale zone and high cytoplasmic nuclear ratio. Mott cells (morular or graped cells) are included in this population. Immature PC showed instead one prominent nucleolus, finely dispersed/vesicular chromatin, a lower cytoplasmic nuclear ratio and a cytoplasm sometimes occupied by small optical empty vesicles. Flaming cells containing a large cytoplasm with several intracytoplasmic vacuoles and binucleated cells were also counted in immature cells.

2.9. Immunofluorescence staining

Sections of 6-μm thickness from paraffin-embedded lymph nodes were processed to detect the ER chaperon BiP and mouse IgG antibodies. Deparaffinized and rehydrated sections were rinsed in Tris 0.1 M, pH 7.6 at 37 °C for 30 min and then incubated with pronase (*Streptomyces griseus*; Sigma-Aldrich, Milan, Italy). Then the sections were blocked with goat serum and horse serum before overnight incubation with the anti-BiP antibody. CY3-labelled goat anti-rabbit IgG (Amersham Bioscences, UK) and fluorescein (isothiocyanate) (FITC)-conjugated horse anti-mouse IgG antibody (DBA, Vector, Italy) were used to detect BiP and intracellular IgG, respectively. A Leica TCS-SL confocal microscope, equipped with Argon and He/Ne laser sources, was used to detect the florescence signal.

2.10. Statistical analysis

Statistical analysis was performed using one-way ANOVA followed by Tukey post-test when 3 experimental groups were compared or Mann Whitney test when 2 experimental groups were compared (GraphPad Software, Inc., La Jolla, CA, USA).

3. Results

3.1. Plasma IgG and IgG isotypes are affected by I-152 treatment

LP-BM5-infected mice develop an unusual proliferation and polyclonal activation of B cells resulting in abnormal Ig production and secretion [3,8]. In agreement with previous findings [8], plasma IgG significantly increased in infected mice (I) at 2 weeks (Fig. 1A), peaked at 5 weeks (Fig. 1B) and then slightly declined at 9 weeks (Fig. 1C). The same trend was observed in infected/treated mice (I + I-152); however, at 5 weeks, IgG levels were significantly lower compared with infected animals (Fig. 1B).

IgG isotypes (IgG1 and IgG2a) displayed a predominance of IgG1 in infected mice, indicating a prevalent humoral immune response, in the early phase of infection (2 weeks) (Fig. 1D), as previously reported [5]. Notably, IgG1 levels were significantly lower in infected/treated mice (I + I-152) compared to infected animals (I), in agreement with the

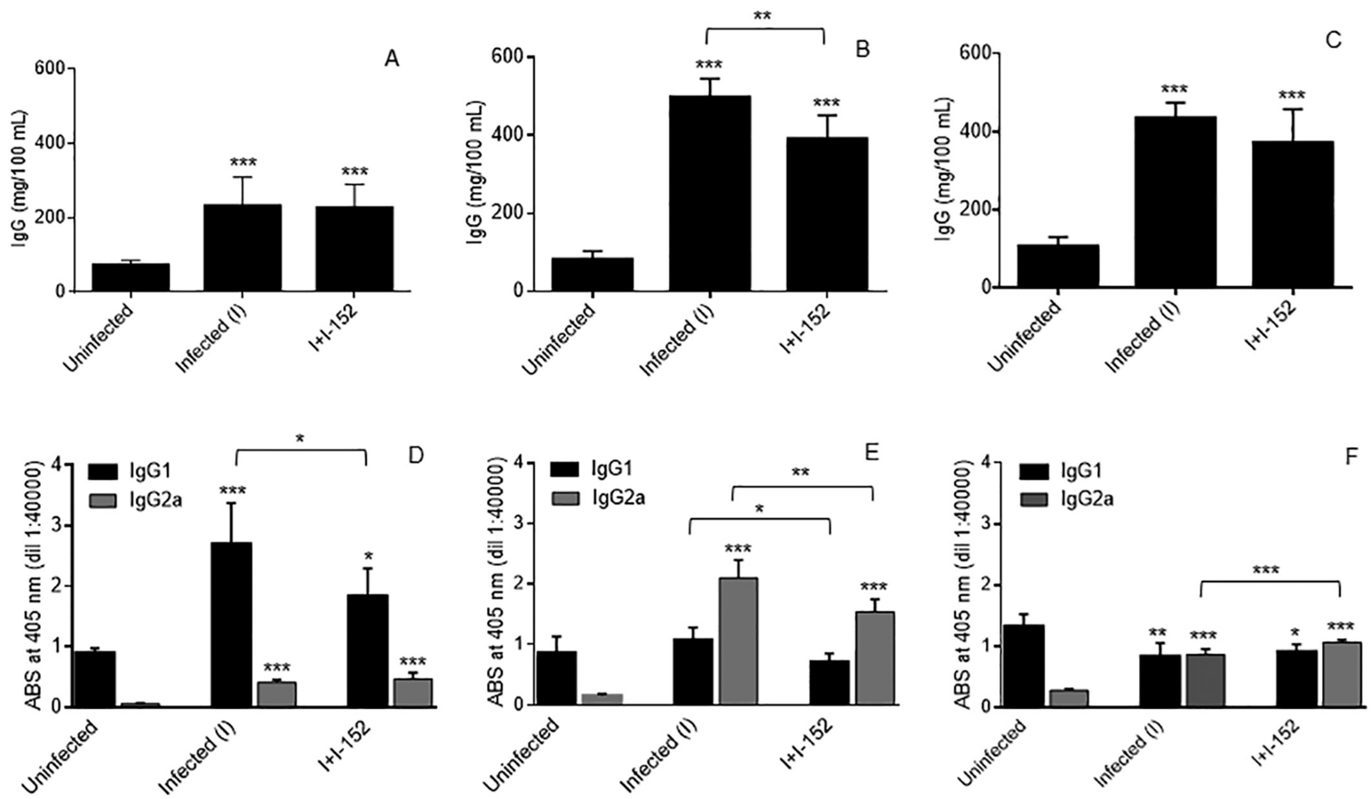

Fig. 1. Plasma IgG (A-C), IgG1 and IgG2a (D-F) in uninfected, infected/untreated (I) and infected/treated (I + I-152) mice. Mice were infected by two successive i.p. injections at 24-h intervals each containing 0.25 units of reverse transcriptase. I-152-treated mice received I-152 intraperitoneally (30 μmoles/mouse), every other day, for a total of 9 weeks. At 2 (A, D), 5 (B, E), and 9 (C, F) weeks after virus inoculation, IgG and IgG isotypes were determined in plasma by a double-sandwich ELISA by using anti-mouse IgG, IgG1 or IgG2a as capture antibody and rabbit anti-mouse HRP-conjugated IgG as detection antibody. Detection was performed by addition of 2,2′-azino-di-(3-ethylbenzothiazoline)-6-sulfonic acid) or ABTS as substrate for horseradish peroxidase (HRP) and absorbance was measured at 405 nm. The values are the mean ± S.D. of 5 animals per group. Mice were from one single experiment. Statistically significant differences are represented as follows: $^*p < .05$, $^{**}p < .01$, $^{***}p < .001$.

propensity of I-152 to induce Th1 driven immune responses [5]. The progression of viral infection (5 weeks) was characterized in both experimental groups by a decrease in IgG1 levels and an increase in IgG2a concentration (Fig. 1E). At 9 weeks, both IgG1 and IgG2a decreased, but interestingly, the Th1 associated IgG2a subtype was slightly higher in infected/treated mice than in the infected ones (Fig. 1F).

3.2. IgG levels in the lymph nodes are affected by I-152 treatment

To investigate the molecular mechanisms underlying the inhibitory effect exerted by I-152 on IgG production/secretion, further analyses were performed on the lymph nodes that represent one of the major sites where B cells are activated to produce and release Ig [34].

As shown in Fig. 2 (A-C), a statistically significant increase in the IgG content was detected at all the time points studied. In agreement with the results obtained in plasma, significantly lower IgG levels were found in the lymph nodes of infected/treated animals (I + I-152) than in infected mice (I) at 5 weeks p.i. (Fig. 2B).

Expression of the PC marker Syndecan-1 [35,36] was significantly increased in infected (I) compared to uninfected mice at 2 and 5 weeks, consistently with the maturation of Ab-producing PC (Fig. 2D, E). By contrast, in the infected/treated mice (I + I-152) Syndecan-1 levels were never significantly different from those detected in the uninfected group (Fig. 2D, E), despite the increase in the IgG content observed (Fig. 2A, B). At 5 weeks, Syndecan-1 staining was significantly lower in infected/treated animals than in infected mice, suggesting that an impairment in PC maturation/survival may occur after I-152 treatment (Fig. 2E). This hypothesis may also explain the drop in the lymph node IgG content detected at the same time point (Fig. 2B).

Interestingly, normalization of IgG levels on Syndecan-1 signal (Fig. 2G-I) resulted in a significant higher value in I + I-152 mice compared to the infected ones at 2 weeks (Fig. 2G), suggesting that the effect of I-152 on PC observed at 5 weeks is preceded by intracellular accumulation of IgG.

An imbalance of the redox state towards a more reducing environment is expected to affect folding of the Ig within the ER, because of an impairment in disulfide bond formation [25–27]. To test this hypothesis, the subcellular localization of IgG in the lymph nodes of LP-BM5-infected mice either untreated or treated with I-152, was evaluated by fractionation of whole homogenates by isopycnic sucrose gradient centrifugation. The results reported in Fig. 3 show that a significant amount of IgG co-localizes with the ER marker BiP (fractions 10–12) in the infected/treated animals (I + I-152), but not in the infected group (I), supporting the idea that I-152 may interfere with IgG folding, leading to IgG accumulation within the ER, and impairing their extracellular secretion [37].

3.3. Activation of ER stress markers is partially affected by I-152 treatment

Maturation and folding of IgG rely on the activity of ER-resident chaperones and folding enzymes, particularly BiP and PDI. BiP has an important role in the folding and assembly of secretory proteins [38,39]; PDI forms and isomerizes disulfide bonds and its concentration in lymphocytes corresponds to their antibody secretion rate [40,41]. The mRNA analysis showed that in infected mice, both I and I + I-152, BiP was induced at 2 weeks, then it further increased at 5 weeks, plateauing at 9 weeks (Fig. 4A). A strong induction of BiP protein expression was also revealed by western blotting analysis; however,

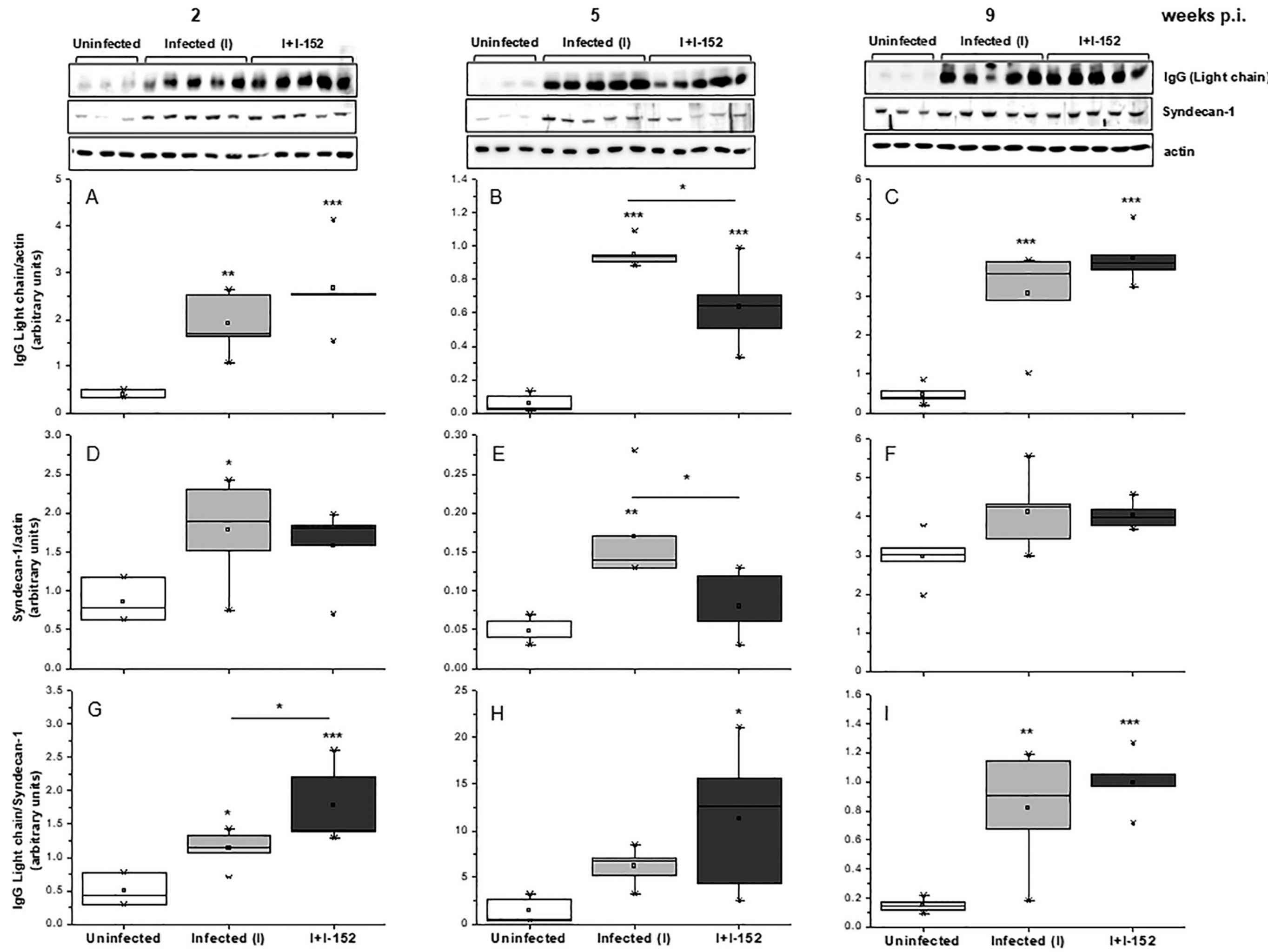

Fig. 2. Western immunoblotting analysis of IgG (A-C) and Syndecan-1 (D-F) levels in the lymph nodes of uninfected, infected/untreated (I) and infected/treated (I + I-152) mice. Lymph nodes were excised at 2, 5 and 9 weeks p.i. After homogenization, lysates were separated on SDS-PAGE gels, transferred to PVDF membrane and probed for the indicated proteins by using specific antibodies. Immunoreactive bands were quantified with the Image Lab software and IgG and Syndecan-1 levels were normalized on actin. Data sets are depicted as boxplots where the open dot indicates the mean and the X-shaped symbol the outliers. In the panels G-I, IgG/Syndecan-1 ratio calculated for each experimental group is reported. For simplicity, only the IgG light chain is shown. Five infected/untreated, 5 infected/treated and at least 3 uninfected mice were analyzed. Mice were from one single experiment. Statistically significant differences are represented as follows: *$p < .05$, **$p < .01$, ***$p < .001$.

differences between the two groups were observed neither at 2 weeks (Fig. 4B) nor at the following time points (not shown).

In the case of PDI, mRNA levels were unchanged after infection, however, protein levels tended to increase in the 2 week-infected mice (I) as compared to the uninfected. Post-transcriptional induction of PDI was abrogated in I-152 treated mice (Fig. 5B).

The UPR pathway plays also a central role in PC development and directs events leading to humoral immunity [19–22,24]. In particular, sXBP-1 regulates the transcription of genes involved in ER expansion, protein folding and synthesis in PC [17,20,21]. sXBP-1 mRNA and protein levels were strongly induced after infection (Fig. 6). A significant reduction in sXBP-1 mRNA and protein contents were observed in infected/treated mice (I + I-152) compared to the infected ones (I) at 5 weeks (Fig. 6A and B, respectively).

Another ER-stress marker strongly up-regulated by infection was CHAC1 which is involved in degradation of cytosolic glutathione in mammalian cells through its γ-glutamylcyclotransferase activity [42]. CHAC1 is specifically induced by UPR activation and is downstream of the PERK/ATF4 signaling cascade [12]. As shown in Fig. 7, differences in CHAC1 mRNA expression were not observed between I and I + I-152 mice; moreover, protein was undetectable at 2 weeks while it was immunostained at 5 and 9 weeks, but its content was not altered by I-152 treatment (not shown). Consistently with this result, the levels of phosphorylated eIF2alpha were not affected by I-152 (not shown).

3.4. PC morphological maturation is affected by I-152 treatment

Lymph node architecture is severely altered by LP-BM5 infection; for this reason, lymph node histopathology has been considered as a useful indicator of disease progression [43,44]. At 2 weeks, differences between infected and uninfected mice were not yet visible and secondary follicles with germinal centers were still present in infected animals (Fig. 8A).

At 5 weeks after infection, the typical lymph node architecture was no longer present in infected mice as the presence of architectural effacement, characterized by cellular monomorphism, prevailed not allowing to distinguish the follicular structures (Fig. 8B). Meanwhile, the number of PC was increased in response to LP-BM5 infection. By contrast, in I-152-treated mice the lymph node architecture, although modified, maintained some characteristics such as the presence of primary follicles (Fig. 8C). An expanded lymphatic sinus network, which could reflect an increased lymph flow through the medullary lymphatic

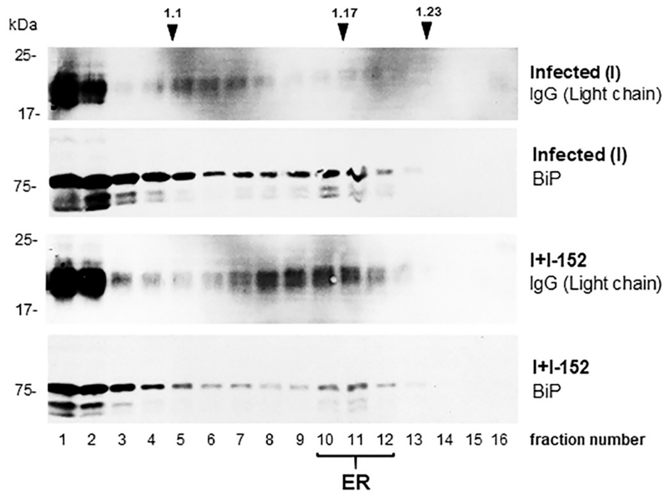

Fig. 3. ER retention of IgG in lymph nodes of infected/untreated (I) and infected/treated (I + I-152) mice. Total proteins extracted from lymph nodes of LP-BM-infected mice either untreated (I) or treated with I-152 for 2 weeks (I + I-152) were fractionated by centrifugation on an isopycnic Suc gradient. Proteins from each fraction were analyzed by SDS-PAGE and immunoblotting using anti-IgG or anti-BiP antiserum. The top of the gradients is on the left; numbers on the top indicate density (g mL^{-1}); numbers on the bottom indicate the gradient fractions. ER fractions are underlined. The positions of molecular mass markers in kD are indicated by numbers on the left of the panels.

sinuses, was observed as well. The histological features of the lymph nodes after 9 weeks of infection were not significantly different from those observed at 5 weeks (not shown).

Particular attention was focused on PC morphology of infected mice (Fig. 8D-G). It is known that excessive amount of proteins, which can neither be secreted nor degraded, can be accumulated into intracytoplasmic spherical inclusions, named Russell bodies [45–47]. At 5 weeks, in all the infected animals, either untreated or treated, we observed several PC containing multiple varied size spherical inclusions, likely Russell bodies structures (Mott cells) (Fig. 8D). To investigate the nature of the inclusions detected in PC of infected mice, we performed double immunofluorescence for IgG and BiP (Fig. 8F, G). When the double labelling was examined simultaneously, there was a blending of the immuno-reactivity merge, suggesting co-localization of both proteins, likely in the ER (Fig. 8F, G yellow arrows). However, in all the infected samples, I-152-treated or not, we observed at all the times investigated, the presence of numerous spherical IgG positive inclusions that did not overlap with BiP positive structures (Fig. 8F, G blue arrows).

Immature PC, having eccentrically placed vesicular nuclei, (clock faced nuclei) (Fig. 8E) and several flamed cells (insert of Fig. 8E) were observed particularly in I-152-treated mice. After 5 weeks of infection, an inverted relationship between immature and mature cells was detected in the lymph nodes of infected and infected/treated mice, as revealed by semiquantitative analysis (Fig. 9B). No differences were found at the other time points investigated (Fig. 9A and C).

4. Discussion

One of the primary events in the development of MAIDS is the infection and polyclonal activation of B cells, resulting in a rapid increase in plasma Ig levels [3].

We have previously demonstrated that I-152 treatment of LP-BM5-infected mice reduces the levels of Th2 cytokines, i.e. IL-4 and IL-5 [5]. These cytokines had been reported to have an important role in promoting humoral immunity and inducing IgG1 antibodies [48,49]. Based on these evidences we hypothesized that I-152 could hinder the signs of the disease by dual mechanisms of action: on the one hand, it can directly hamper viral replication as previously demonstrated [5,30,50] and here confirmed by evaluation of the disease parameters and quantification of the lymph node viral load (data not shown); on the other hand, in the early phases of infection it regulates the induction of IL-12 and Th1/Th2 cytokine production by modulating intra-macrophage glutathione-redox status [5]. Consistent with this hypothesis, herein we show that I-152 treatment reduces IgG1 titer at 2 weeks p.i., supporting the conclusion that I-152 shifts the ratio Th1/Th2 towards Th1. It would be interesting to investigate how I-152 treatment impacts on LP-BM5-specific antibody responses and whether the redox state can also have a role in the development and/or function of T follicular helper (Tfh) cells, which have emerged as an important cell type

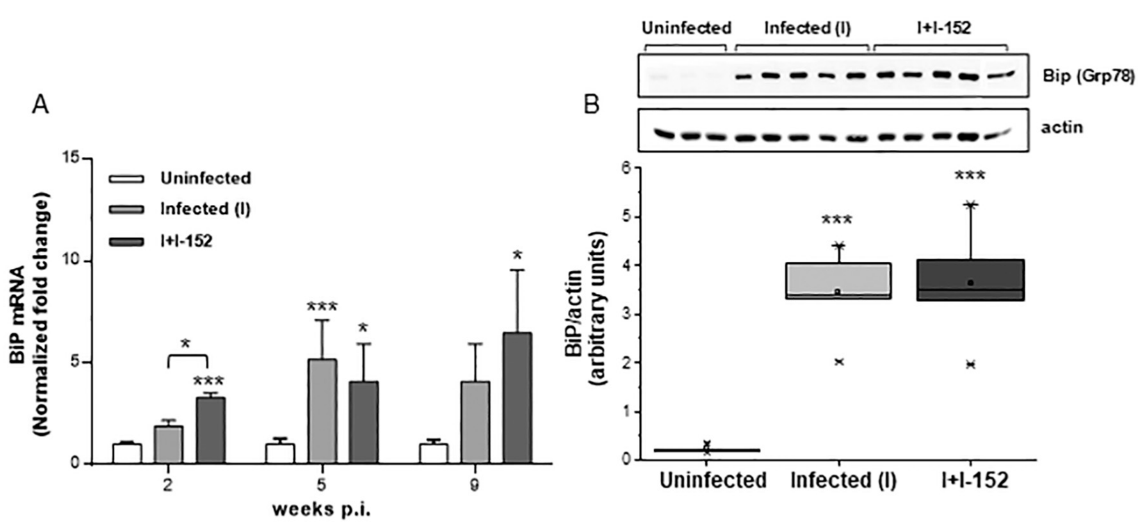

Fig. 4. BiP expression in the lymph nodes of uninfected, infected/untreated (I) and infected/treated (I + I-152) mice. (A) Lymph nodes were excised at 2, 5 and 9 weeks p.i. After total RNA extraction and cDNA synthesis, relative mRNA expression was determined by real-time PCR with the 2-ΔΔCt method using β-2 microglobulin (B2M) as a reference gene and uninfected mice as calibrator. The values are the mean ± S.D. of at least 3 animals per group. (B) protein extracts (5 μgs) obtained from mouse lymph nodes excised at 2 weeks p.i. were resolved onto a 10% SDS polyacrylamide gel and immunoblotted with an anti BiP antibody. BiP levels were normalized on actin and values depicted as boxplot where the open dot indicates the mean and the X-shaped symbol the outliers. Five infected/untreated, 5 infected/treated and at least 3 uninfected mice were analyzed. Mice were from one single experiment. Statistically significant differences are represented as follows: $^*p < .05$, $^{**}p < .01$, $^{***}p < .001$.

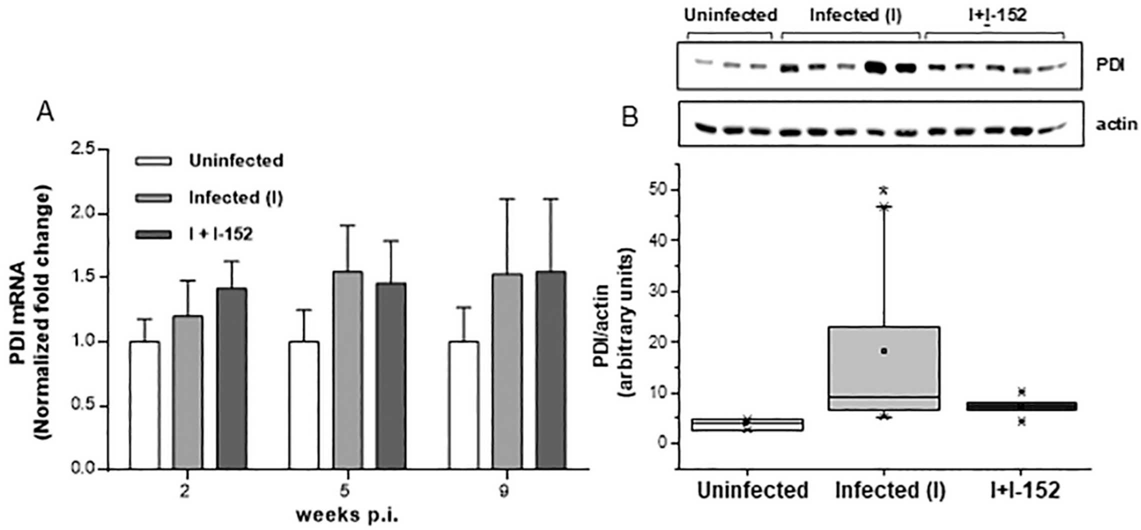

Fig. 5. PDI expression in the lymph nodes of uninfected, infected/untreated (I) and infected/treated (I + I-152) mice. (A) Lymph nodes were excised at 2, 5 and 9 weeks p.i. After total RNA extraction and cDNA synthesis, relative mRNA expression was determined by real-time PCR with the 2-ΔΔCt method using β-2 microglobulin (B2M) as a reference gene and uninfected mice as calibrator. The values are the mean ± S.D. of at least 3 animals per group. (B) protein extracts (5 μgs) obtained from mouse lymph nodes excised at 2 weeks p.i. were resolved onto a 10% SDS polyacrylamide gel and immunoblotted with an anti PDI antibody. PDI levels were normalized on actin and values depicted as boxplot where the open dot indicates the mean and the X-shaped symbol the outliers. Five infected/untreated, 5 infected/treated and at least 3 uninfected mice were analyzed. Mice were from one single experiment. *$p < .05$.

required for the formation of germinal centers and related B cells responses [51].

However, these data appear to indicate that the lower plasma IgG levels measured in infected I-152-treated animals may be the consequence of a further mechanism by which I-152 affects the later phases of the disease (i.e. 5 weeks p.i.) characterized by rapid B cell proliferation and high frequency of Ig-secreting cells [8]. Data presented show that I-152 modulates the antibody-mediated immune response by impairing the secretory capacity as well as the maturation of PC. These cells are particularly dependent on the ER quality control system to ensure that only correctly assembled Ig molecules are transported to the cell surface. The results reported in this paper show that in the lymph nodes of infected mice treated with I-152, a great quantity of IgG is indeed retained within the PC at 2 weeks p.i and in part accumulated in the ER. It is well known that the ER resident chaperons BiP and PDI act synergistically to fold Ig. In agreement with these observations, BiP expression was strongly induced after infection with no significant differences between the untreated and treated groups. Conversely, PDI protein levels were higher in the lymph nodes of infected mice but not in I-152-treated mice at 2 weeks p.i., despite the fact that PDI mRNA

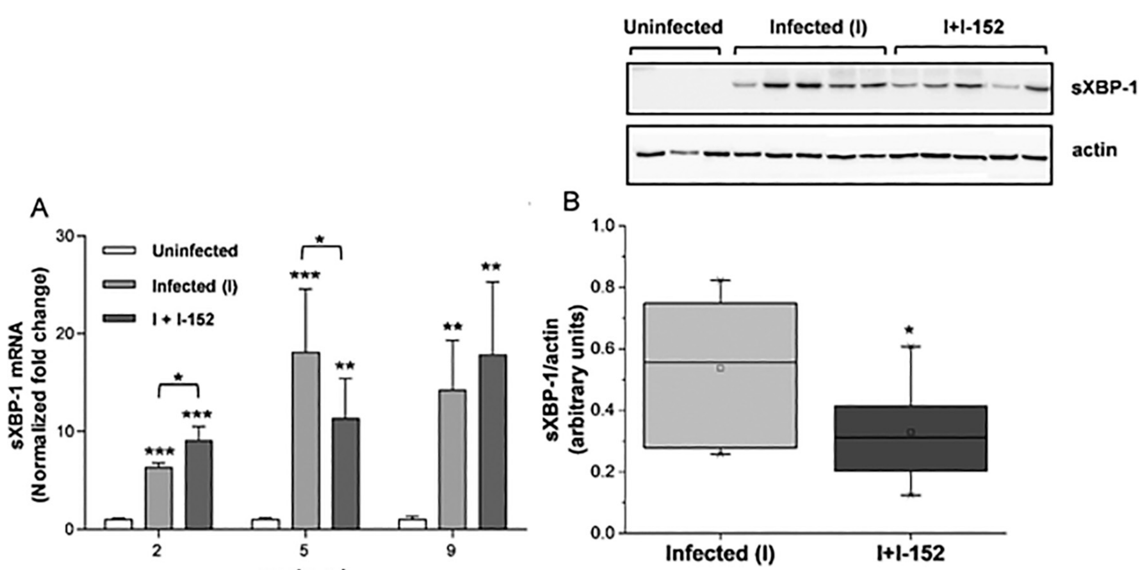

Fig. 6. sXBP-1 expression in the lymph nodes of uninfected, infected/untreated (I) and infected/treated (I + I-152) mice. (A) Lymph nodes were excised at 2, 5 and 9 weeks p.i. After total RNA extraction and cDNA synthesis, relative mRNA expression was determined by real-time PCR with the 2-ΔΔCt method using β-2 microglobulin (B2M) as a reference gene and uninfected mice as calibrator. The values are the mean ± S.D. of at least 3 animals per group. (B) protein extracts (20 μgs) obtained from mouse lymph nodes excised at 5 weeks p.i. were resolved onto a 10% SDS polyacrylamide gel and immunoblotted with an antibody which recognizes the spliced XBP-1 isoform (sXBP-1). sXBP-1 levels were normalized on actin and values depicted as boxplot where the open dot indicates the mean and the X-shaped symbol the outliers. Five infected/untreated and infected/treated mice were analyzed. Mice were from one single experiment. Statistically significant differences are represented as follows: *$p < .05$, **$p < .01$, ***$p < .001$.

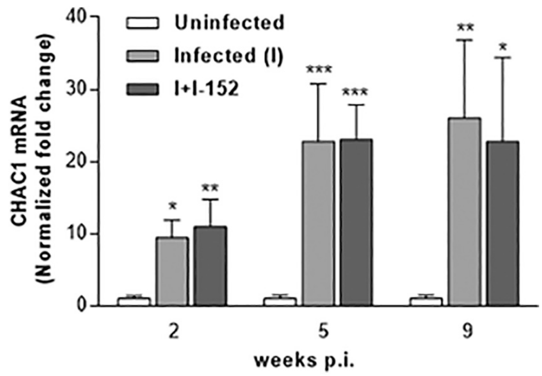

Fig. 7. CHAC1 expression in the lymph nodes of uninfected, infected/untreated (I) and infected/treated (I + I-152) mice. Lymph nodes were excised at 2, 5 and 9 weeks p.i. After total RNA extraction and cDNA synthesis, relative mRNA expression was determined by real-time PCR with the 2-ΔΔCt method using β-2 microglobulin (B2M) as a reference gene and uninfected mice as calibrator. The values are the mean ± S.D. of at least 3 animals per group. Statistically significant differences are represented as follows: $^*p < .05$, $^{**}p < .01$, $^{***}p < .001$.

levels were neither increased following infection nor affected by I-152. These data suggest that PDI protein levels augmented through post-transcriptional mechanisms in infected mice to support a higher demand of IgG folding, and that this event was affected by I-152 treatment, leading to IgG accumulation. It has been suggested that PDI turnover may be related to the redox state of the cell [52]. Moreover, I-152 treatment could influence the redox-sensitive cysteines that have been widely demonstrated to be important for its activity [53,54]. The more oxidative environment created by GSH depletion during LP-BM5 infection [5] would favour oxidation of PDI and disulfide bond formation which could be impaired by the more reduced environment created by I-152. In support to this hypothesis, it has been previously demonstrated that an increase in the intracellular GSH content interferes with the PDI-dependent maturation of influenza virus hemagglutinin [55], and that in vivo up-regulation of PDI induced by influenza infection can be counterbalanced by GSH increase [56]. Interestingly, accumulation of IgG in the PC observed in the early phases of infection (i.e. 2 weeks p.i.) was followed by a drastic drop in plasma and intracellular IgG levels found at later times (i.e. 5 weeks p.i.) where the ability of I-152 to affect PC maturation was clearly evident. In fact, while lymph node architecture was partially preserved by 152

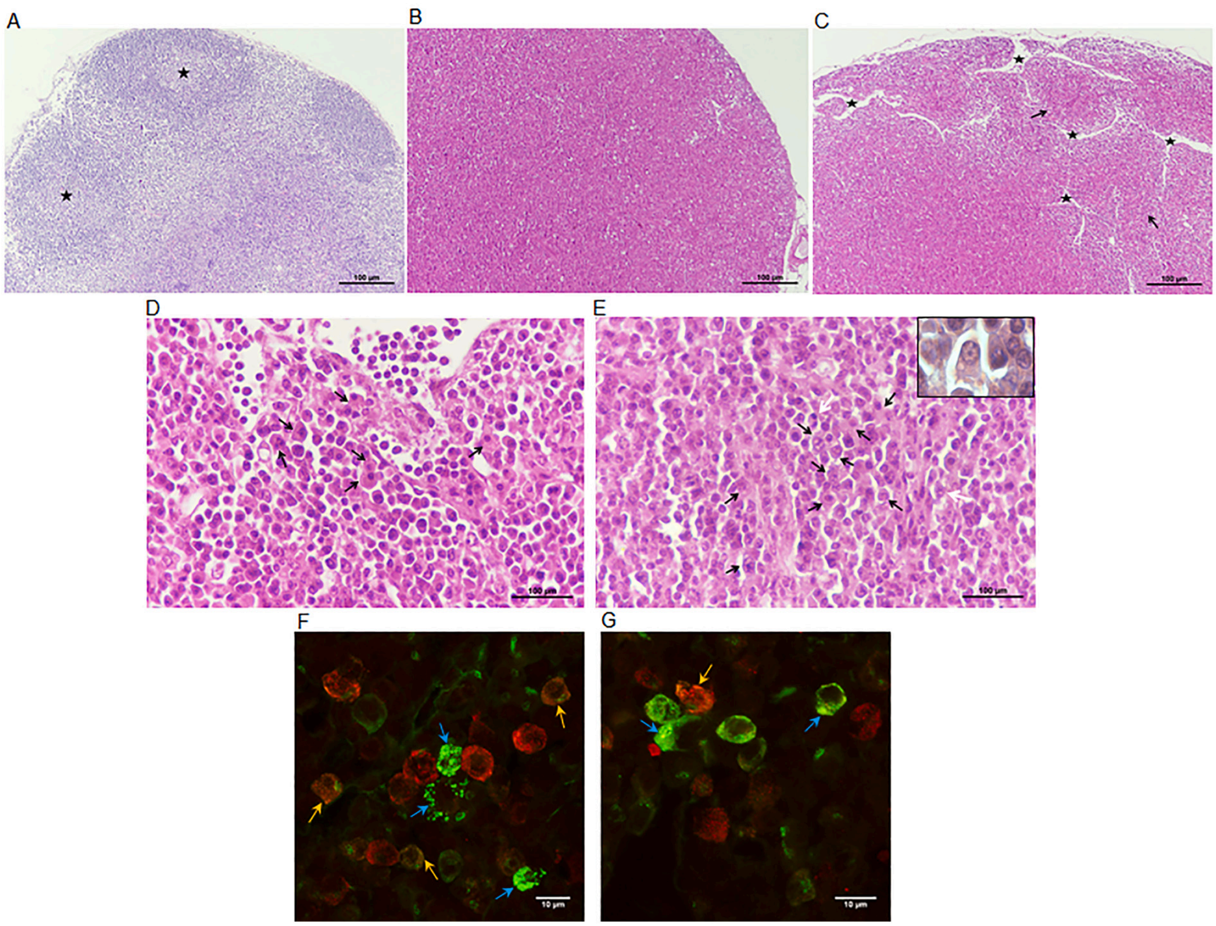

Fig. 8. Hematoxylin and eosin (H&E) staining of sections of lymph nodes of infected/untreated (I) and infected/treated (I + I-152) mice (A-E) and immunofluorescence staining of section of lymph nodes of infected/untreated (I) and infected/treated mice (I + I-152) (F, G).

At 2 weeks p.i., follicles with germinal centers (asterisks) are still visible (A).

At 5 weeks p.i., in mice belonging to the infected/untreated group the normal histological architecture was replaced by a monomorphic population of lymphocytes (B). Several mature PC, including Mott cells containing numerous Russel bodies (arrows) were present (D).

At 5 weeks p.i., in infected/treated mice, the presence of follicular structures (arrows) and expanded lymphatic sinus (asterisks) were observed (C). Undifferentiated PC containing vesicular chromatin often presenting intracytoplasmic vacuoles (black arrows) and binucleated cells (white arrows) predominated (E); flamed cell (insert).

At 5 weeks p.i., in infected/treated (F) and infected/untreated (G) mice IgG (green) colocalize with BiP (red) (yellow arrows) or are accumulated in Russell bodies-like structures (blue arrows).

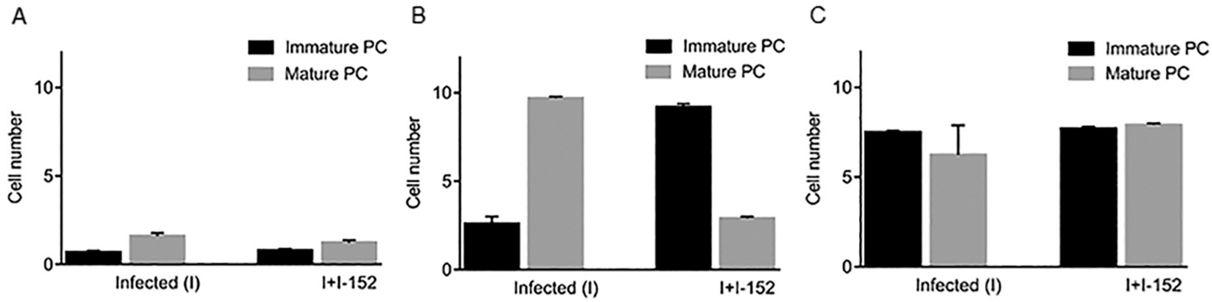

Fig. 9. Immature and mature PC in the lymph nodes of infected/untreated (I) and infected/treated (I + I-152) mice. Semiquantitative cell counts were performed in H&E stained sections of lymph nodes at 2 (A), 5 (B) and 9 (C) weeks p.i. The cell number represents the average of the counts of the PC performed at 40× magnification in 5 microscopic fields/mouse. Three infected/untreated and 3 infected/treated mice were analyzed. Mice were from one single experiment.

treatment, a lower quantity of mature PC was present as suggested by Syndecan-1 quantification and confirmed by a semiquantitative scoring method for mouse model histopathology [57]. Differentiation of B cells into PC requires some morphological changes, which guarantee increased capacity of Ab synthesis and secretion, such as expansion of cytoplasm and ER as well as decrease in nuclear area. The splicing of XBP-1 is induced during PC differentiation in response to Th2 cytokines, such as IL-4, and this event up-regulates Ig gene transcription leading the PC to synthesize and secrete antibodies [22,24,58,59]. Fewer mature PC in treated mice are compatible with the decreased expression of sXBP-1 found in the lymph nodes of these animals. The defective expression of sXBP-1 can undoubtedly affect the differentiation of a PC, but it has also been demonstrated that blockade of the IRE1α-XBP-1 pathway contributes to the death of myeloma cells under ER stress conditions [60]. Thus, secretory cells that require an active UPR to ensure proper processing of proteins in the ER may be particularly susceptible to apoptosis by agents that evoke ER stress but impair the UPR. Hence, inhibition of IRE1α-XBP-1 signaling and increased amount of misfolded/unfolded IgG caused by I-152 treatment could ultimately induce death of PC that are particularly sensitive to this effect due to their high levels of Ab production [61].

Moreover, in all the infected animals, either untreated or treated, despite the activation of UPR branches, likely to cope with Ig over expression, a cellular indigestion caused by an excessive quantity of unfolded IgG, not proceeding along the secretory pathway, occurs. This conclusion is supported by the presence in PC of numerous Russell bodies-like vesicles [47]. As previously proposed by Valetti et al. [47], these bodies filled with Ig seem to be an “emergency” response of the cell to accumulation of unfolded Ig. Although most commonly found in patients with multiple myeloma, Russell bodies don't necessarily correspond to malignant changes of PC, but they can be associated with sustained immunologic stimulation and/or inflammation in association with abnormal synthesis, trafficking, or excretion of the Ig [62]. Several ER-storage diseases are characterized by the formation of inclusion bodies where mutated or unfolded proteins are sequestered outside the secretory pathway. These bodies are membrane-limited and seem different from autophagosomes or lysosomes [63].

The presence of loads of unfolded or misfolded proteins is common during viral infection [64] and, as expected, LP-BM5 infection resulted in the induction of UPR activation. Among the up-regulated mRNAs, ChaC glutathione-specific γ-glutamylcyclotransferase 1 (CHAC1) showed dramatically increased expression (about 20 times over basal levels at 5 weeks p.i.). Various stimuli that trigger ER stress, including infection, have been reported to upregulate CHAC1 mRNA expression and consequent depletion of cellular GSH levels and accumulation of ROS [65]. Several mechanisms by which different viruses induce a decrease in GSH content have been described [66]. Thus, we suggest that increased expression of CHAC1 could be one important factor leading to GSH depletion in LP-BM5 infection, presumably to make the environment suitable for correct protein folding and virus replication. Notably, I-152 treatment did not affect CHAC1 expression, suggesting that in this experimental model the molecule can raise intracellular GSH levels by providing precursors to synthesize GSH and/or by influencing the pathways involved in GSH synthesis rather than affect GSH degradation.

The data show that a further mechanism by which I-152 could inhibit IgG production during LP-BM5 infection is by inducing perturbation in ER redox state leading to impaired IgG folding/secretion as well as to reduced maturation and, probably survival, of PC (Fig. 10).

Conclusions. Intracellular redox state has a key role in folding and secretion of Ig as well as in maturation of PC where UPR is highly activated. Compounds that shift the intracellular environment towards a more reduced state affect PDI and sXBP1 expression. These molecules may be potential therapeutic agents for the treatment of multiple myeloma and other tumours that originate from secretory cells.

CRediT authorship contribution statement

Fraternale Alessandra: Writing - original draft, Investigation, Formal analysis, Writing - review & editing, Visualization, Supervision, Methodology, Conceptualization, Funding acquisition. **Zara Carolina:** Investigation, Formal analysis. **Di Mambro Tomas:** Investigation, Formal analysis. **Manuali Elisabetta:** Investigation, Formal analysis, Writing - review & editing. **Genovese Domenica Anna:** Investigation, Formal analysis. **Galluzzi Luca:** Investigation, Formal analysis, Writing - review & editing. **Diotallevi Aurora:** Investigation, Formal analysis. **Pompa Andrea:** Investigation, Formal analysis, Writing - review & editing. **De Marchis Francesca:** Investigation, Formal analysis, Writing - review & editing. **Ambrogini Patrizia:** Investigation, Formal analysis. **Cesarini Erica:** Investigation, Formal analysis. **Luchetti Francesca:** Investigation, Formal analysis. **Smietana Michaël:** Writing - review & editing. **Green Kathy:** Writing - review & editing. **Bartoccini Francesca:** Writing - review & editing. **Magnani Mauro:** Writing - review & editing, Funding acquisition. **Crinelli Rita:** Investigation, Formal analysis, Writing - review & editing, Visualization, Supervision, Methodology, Conceptualization.

Declaration of competing interest

The authors declare that they have no known competing financial interests or personal relationships that could have appeared to influence the work reported in this paper.

Acknowledgements

This work was funded by Ministero dell'Istruzione, dell'Università e della Ricerca (MIUR) (PRIN [Research Projects of National Interest] 2010-2011-prot. 2010PHT9NF_004). Furthermore, we are grateful to University of Urbino Carlo Bo for partial financial support to this research.

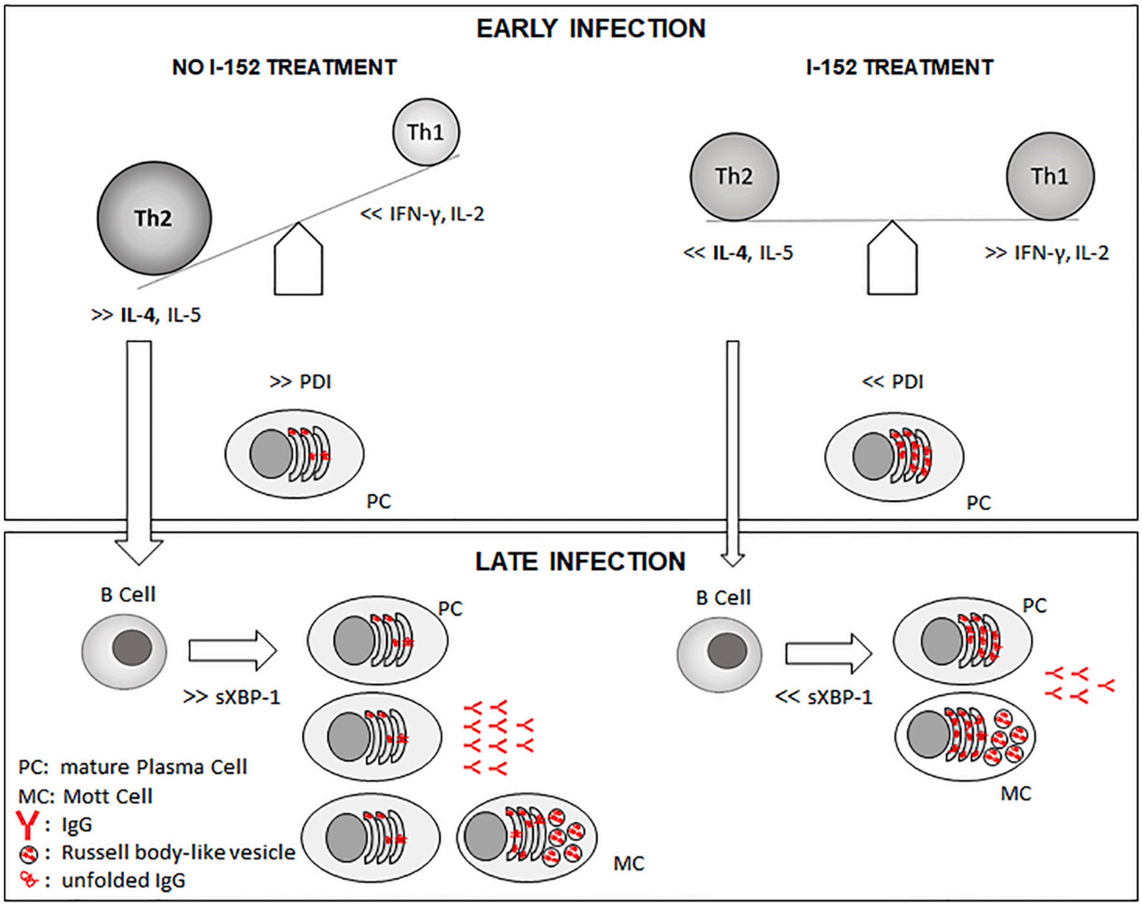

Fig. 10. I-152 immunomodulatory effects in LP-BM5 infection. During the early LP-BM5 infection, I-152 treatment influences Th1/Th2 cytokine production in favour of Th1 [5] and accumulates unfolded IgG inside the ER (above). During the late LP-BM5 infection, I-152 treatment impairs differentiation and secretory capacity of PC (below).

References

[1] J.W. Hartley, T.N. Fredrickson, R.A. Yetter, M. Makino, H.C. Morse 3rd, Retrovirus-induced murine acquired immunodeficiency syndrome: natural history of infection and differing susceptibility of inbred mouse strains, J. Virol. 63 (1989) 1223–1231.

[2] S.P. Klinken, T.N. Fredrickson, J.W. Hartley, R.A. Yetter, H.C. Morse 3rd, Evolution of B cell lineage lymphomas in mice with a retrovirus induced immunodeficiency syndrome, MAIDS, J. Immunol. 140 (1988) 1123–1131.

[3] D.E. Mosier, R.A. Yetter, H.C. Morse 3rd, Retroviral induction of acute lymphoproliferative disease and profound immunosuppression in adult C57BL/6 mice, J. Exp. Med. 161 (1985) 766–784, https://doi.org/10.1084/jem.161.4.766.

[4] D.E. Mosier, Animal models for retrovirus-induced immunodeficiency disease, Immunol. Investig. 15 (1986) 233–261, https://doi.org/10.3109/08820138609026687.

[5] S. Brundu, L. Palma, G.G. Picceri, D. Ligi, C. Orlandi, L. Galluzzi, L. Chiarantini, A. Casabianca, G.F. Schiavano, M. Santi, F. Mannello, K. Green, M. Smietana, M. Magnani, A. Fraternale, Glutathione depletion is linked with Th2 polarization in mice with a retrovirus-induced immunodeficiency syndrome, murine AIDS: role of proglutathione molecules as immunotherapeutics, J. Virol. 90 (2016) 7118–7130, https://doi.org/10.1128/JVI.00603-16.

[6] R.T. Gazzinelli, M. Makino, S.K. Chattopadhyay, C.M. Snapper, A. Sher, A.W. Hügin, H.C. Morse 3rd, CD4- subset regulation in viral infection. Preferential activation of Th2 cells during progression of retrovirus induced immunodeficiency in mice, J. Immunol. 148 (1992) 182–188.

[7] A. Sher, R.T. Gazzinelli, I.P. Oswald, M. Clerici, M. Kullberg, E.J. Pearce, J.A. Berzofsky, T.R. Mosmann, S.L. James, H.C. Morse 3rd, Role of T-cell derived cytokines in the downregulation of immune responses in parasitic and retroviral infection, Immunol. Rev. 127 (1992) 183–204, https://doi.org/10.1111/j.1600-065x.1992.tb01414.x.

[8] D.M. Klinman, H.C. Morse 3rd, Characteristics of B cell proliferation and activation in murine AIDS, J. Immunol. 142 (1989) 1144–1149.

[9] J.N. Gass, N.M. Gifford, J.W. Brewer, Activation of an unfolded protein response during differentiation of antibody-secreting B cells, J. Biol. Chem. 277 (2002) 49047–49054, https://doi.org/10.1074/jbc.M205011200.

[10] Y. Ma, Y. Shimizu, M.J. Mann, Y. Jin, L.M. Hendershot, PC differentiation initiates a limited ER stress response by specifically suppressing the PERK-dependent branch of the unfolded protein response, Cell Stress Chaperones 15 (2010) 281–293, https://doi.org/10.1007/s12192-009-0142-9.

[11] L. Zhang, A. Wang, Virus-induced ER stress and the unfolded protein response, Front. Plant Sci. 3 (2012) 293, https://doi.org/10.3389/fpls.2012.0029.

[12] L. Galluzzi, A. Diotallevi, M. Magnani, Endoplasmic reticulum stress and unfolded protein response in infection by intracellular parasites, Future Sci. OA 3 (2017) FSO198, , https://doi.org/10.4155/fsoa-2017-0020.

[13] M.J. Feige, L.M. Hendershot, J. Buchner, How antibodies fold, Trends Biochem. Sci. 35 (2010) 189–198, https://doi.org/10.1016/j.tibs.2009.11.005.

[14] J.N. Gass, K.E. Gunn, R. Sriburi, J.W. Brewer, Stressed-out B cells? Plasma-cell differentiation and the unfolded protein response, Trends Immunol. 25 (2004) 17–24, https://doi.org/10.1016/j.it.2003.11.004.

[15] A.M. Reimold, N.N. Iwakoshi, J. Manis, P. Vallabhajosyula, E. Szomolanyi-Tsuda, E.M. Gravallese, D. Friend, M.J. Grusby, F. Alt, L.H. Glimcher, PC differentiation requires the transcription factor XBP-1, Nature 412 (2001) 300–307, https://doi.org/10.1038/35085509.

[16] J. Grootjans, A. Kaser, R.J. Kaufman, R.S. Blumberg, The unfolded protein response in immunity and inflammation, Nat. Rev. Immunol. 16 (2016) 469–484, https://doi.org/10.1038/nri.2016.62.

[17] K. Lee, W. Tirasophon, X. Shen, M. Michalak, R. Prywes, T. Okada, H. Yoshida, K. Mori, R.J. Kaufman, IRE1-mediated unconventional mRNA splicing and S2P-mediated ATF6 cleavage merge to regulate XBP1 in signaling the unfolded protein response, Genes Dev. 16 (2002) 452–466, https://doi.org/10.1101/gad.964702.

[18] H. Yoshida, T. Matsui, A. Yamamoto, T. Okada, K. Mori, XBP1 mRNA is induced by ATF6 and spliced by IRE1 in response to ER stress to produce a highly active transcription factor, Cell 107 (2001) 881–891, https://doi.org/10.1016/s0092-8674(01)00611-0.

[19] A.H. Lee, G.C. Chu, N.N. Iwakoshi, L.H. Glimcher, XBP-1 is required for biogenesis of cellular secretory machinery of exocrine glands, EMBO J. 24 (2005) 4368–4380, https://doi.org/10.1038/sj.emboj.7600903.

[20] A.L. Shaffer, M. Shapiro-Shelef, N.N. Iwakoshi, A.H. Lee, S.B. Qian, H. Zhao, X. Yu, L. Yang, B.K. Tan, A. Rosenwald, E.M. Hurt, E. Petroulakis, N. Sonenberg, J.W. Yewdell, K. Calame, L.H. Glimcher, L.M. Staudt, XBP1, downstream of Blimp-1, expands the secretory apparatus and other organelles, and increases protein synthesis in PC differentiation, Immunity 21 (2004) 81–93, https://doi.org/10.1016/j.immuni.2004.06.010.

[21] H. Zhu, B. Bhatt, S. Sivaprakasam, Y. Cai, S. Liu, S.K. Kodeboyina, N. Patel,

N.M. Savage, A. Sharma, R.J. Kaufman, H. Li, N. Singh, Ufbp1 promotes PC development and ER expansion by modulating distinct branches of UPR, Nat. Commun. 10 (2019) 1084, https://doi.org/10.1038/s41467-019-08908-5.

[22] N.N. Iwakoshi, A.H. Lee, P. Vallabhajosyula, K.L. Otipoby, K. Rajewsky, L.H. Glimcher, PC differentiation and the unfolded protein response intersect at the transcription factor XBP-1, Nat. Immunol. 4 (2003) 321–329, https://doi.org/10.1038/ni907.

[23] J.S. So, Roles of endoplasmic reticulum stress in immune responses, Mol. Cells 41 (2018) 705–716. doi:10.14348/molcells.2018.0241.

[24] N. Taubenheim, D.M. Tarlinton, S. Crawford, L.M. Corcoran, P.D. Hodgkin, S.L. Nutt, High rate of antibody secretion is not integral to plasma cell differentiation as revealed by XBP-1 deficiency, J. Immunol. 189 (2012) 3328–3338, https://doi.org/10.4049/jimmunol.1201042.

[25] W.C. Chong, M.D. Shastri, R. Eri, Endoplasmic reticulum stress and oxidative stress: a vicious nexus implicated in bowel disease pathophysiology, Int. J. Mol. Sci. 18 (2017) 771, https://doi.org/10.3390/ijms18040771.

[26] V. Plaisance, S. Brajkovic, M. Tenenbaum, D. Favre, H. Ezanno, A. Bonnefond, C. Bonner, V. Gmyr, J. Kerr-Conte, B.R. Gauthier, C. Widmann, G. Waeber, F. Pattou, P. Froguel, A. Abderrahmani, Endoplasmic reticulum stress links oxidative stress to impaired pancreatic beta-cell function caused by human oxidized LDL, PLoS One 11 (2016) e0163046, , https://doi.org/10.1371/journal.pone.0163046.

[27] J. Wang, K.A. Pareja, C.A. Kaiser, C.S. Sevier, Redox signaling via the molecular chaperone BiP protects cells against endoplasmic reticulum-derived oxidative stress, Elife J3 (2014) e03496, , https://doi.org/10.7554/eLife.03496.

[28] S. Chakravarthi, N.J. Bulleid, Glutathione is required to regulate the formation of native disulfide bonds within proteins entering the secretory pathway, J. Biol. Chem. 279 (2004) 39872–39879, https://doi.org/10.1074/jbc.M406912200.

[29] R. Crinelli, C. Zara, M. Smietana, M. Retini, M. Magnani, A. Fraternale, Boosting GSH using the co-drug approach: I-152, a conjugate of N-acetyl-cysteine and β-mercaptoethylamine, Nutrients 11 (2019) 1291, https://doi.org/10.3390/nu11061291.

[30] J. Oiry, P. Mialocq, J.Y. Puy, P. Fretier, N. Dereuddre-Bosquet, D. Dormont, J.L. Imbach, P. Clayette, Synthesis and biological evaluation in human monocyte-derived macrophages of N-(N-acetyl-L-cysteinyl)-S-acetylcysteamine analogues with potent antioxidant and anti-HIV activities, J. Med. Chem. 47 (2004) 1789–1795, https://doi.org/10.1021/jm030374d.

[31] A. Fraternale, M.F. Paoletti, S. Dominici, A. Caputo, A. Castaldello, E. Millo, E. Brocca-Cofano, M. Smietana, P. Clayette, J. Oiry, U. Benatti, M. Magnani, The increase in intra-macrophage thiols induced by new pro-GSH molecole directs the Th1 skewing in ovalbumin immunized mice, Vaccine 28 (2010) 7676–7682, https://doi.org/10.1016/j.vaccine.2010.09.033.

[32] L. Galluzzi, A. Diotallevi, M. De Santi, M. Ceccarelli, F. Vitale, G. Brandi, M. Magnani, Leishmania infantum induces mild unfolded protein response in infected macrophages, PLoS One 11 (2016) e0168339, , https://doi.org/10.1371/journal.pone.0168339.

[33] M. De Santi, G. Baldelli, A. Diotallevi, L. Galluzzi, G.F. Schiavano, G. Brandi, Metformin prevents cell tumorigenesis through autophagy-related cell death, Sci. Rep. 9 (2019) 66, https://doi.org/10.1038/s41598-018-37247-6.

[34] K.A. Pape, D.M. Catron, A.A. Itano, M.K. Jenkins, The humoral immune response is initiated in lymph nodes by B cells that acquire soluble antigen directly in the follicles, Immunity 26 (2007) 491–502, https://doi.org/10.1016/j.immuni.2007.02.011.

[35] R.D. Sanderson, P. Lalor, M. Bernfield, B lymphocytes express and lose syndecan at specific stages of differentiation, Cell. Regul. 1 (1989) 27–35, https://doi.org/10.1091/mbc.1.1.27.

[36] J. Tellier, S.L. Nutt, Standing out from the crowd: how to identify PC, Eur. J. Immunol. 47 (2017) 1276–1279, https://doi.org/10.1002/eji.201747168.

[37] F. De Marchis, C. Balducci, A. Pompa, H.M. Riise Stensland, M. Guaragno, R. Pagiotti, A.R. Menghini, E. Persichetti, T. Beccari, M. Bellucci, Human α-mannosidase produced in transgenic tobacco plants is processed in human α-mannosidosis cell lines, Plant Biotechnol. J. 9 (2011) 1061–1073, https://doi.org/10.1111/j.1467-7652.2011.00630.x.

[38] M.J. Gething, J. Sambrook, Protein folding in the cell, Nature. 355 (1992) 33–45, https://doi.org/10.1038/355033a0.

[39] L.M. Hendershot, Immunoglobulin heavy chain and binding protein complexes are dissociated in vivo by light chain addition, J. Cell Biol. 111 (1990) 829–837, https://doi.org/10.1083/jcb.111.3.829.

[40] R.B. Freedman, T.R. Hirst, M.F. Tuite, Protein disulfide isomerase: building bridges in protein folding, Trends Biochem. Sci. 19 (1994) 331–336, https://doi.org/10.1016/0968-0004(94)90072-8.

[41] R.A. Roth, M.E. Koshland, Role of disulfide interchange enzyme in immunoglobulin synthesis, Biochemistry 20 (1981)6594–6599. doi:https://doi.org/10.1021/bi00526a012.

[42] A. Kumar, S. Tikoo, S. Maity, S. Sengupta, S. Sengupta, A. Kaur, A.K. Bachhawat, Mammalian proapoptotic factor ChaC1 and its homologues function as γ-glutamyl cyclotransferases acting specifically on glutathione, EMBO Rep. 13 (2012) 1095–1101, https://doi.org/10.1038/embor.2012.156.

[43] L.C. Clouser, C.M. Holtz, M. Mullett, D.L. Crankshaw, J.E. Briggs, M.G. O'Sullivan, S.E. Patterson, L.M. Mansky, Activity of a novel combined antiretroviral therapy of gemcitabine and decitabine in a mouse model for HIV-1, Antimicrob. Agents Chemother. 56 (2012) 1942–1948, https://doi.org/10.1128/AAC.06161-11.

[44] R.A. Yetter, R.M. Buller, J.S. Lee, K.L. Elkins, D.E. Mosier, T.N. Fredrickson, H.C. Morse 3rd, CD4+ T cells are required for development of a murine retrovirus-induced immunodeficiency syndrome (MAIDS), J. Exp. Med. 168 (1988) 623–635, https://doi.org/10.1084/jem.168.2.623.

[45] R.R. Kopito, R. Sitia, Aggresomes and Russell bodies, symptoms of cellular indigestion? EMBO Rep. 1 (2000) 225–231, https://doi.org/10.1093/embo-reports/kvd052.

[46] J. Stoops, S. Byrd, H. Hasegawa, Russell body inducing threshold depends on the variable domain sequences of individual human IgG clones and the cellular protein homeostasis, Biochim. Biophys. Acta 1823 (2012) 1643–1657, https://doi.org/10.1016/j.bbamcr.2012.06.015.

[47] C. Valetti, C.E. Grossi, C. Milstein, R. Sitia, Russell bodies: a general response of secretory cells to synthesis of a mutant immunoglobulin which can neither exit from, nor be degraded in, the endoplasmic reticulum, J. Cell Biol. 115 (1991) 983–994, https://doi.org/10.1083/jcb.115.4.983.

[48] B.J. Kim, B.R. Kim, Y.H. Kook, B.J. Kim, Potential of recombinant mycobacterium paragordonae expressing HIV Gag as a prime vaccine for HIV infection, Sci. Rep. 9 (2019) 15515, https://doi.org/10.1038/s41598-019-51875-6.

[49] A.R. Mathers, C.F. Cuff, Role of interleukin-4 (IL-4) and IL-10 in serum immunoglobulin G antibody responses following mucosal or systemic reovirus infection, J. Virol. 78 (2004) 3352–3360, https://doi.org/10.1128/jvi.78.7.3352-3360.2004.

[50] A. Fraternale, M.F. Paoletti, A. Casabianca, C. Orlandi, G.F. Schiavano, L. Chiarantini, P. Clayette, J. Oiry, J.-U. Vogel, J. Cinatl Jr., M. Magnani, Inhibition of murine AIDS by pro-glutathione (GSH) molecules, Antivir. Res. 77 (2008) 120–127, https://doi.org/10.1016/j.antiviral.2007.11.004.

[51] S. Crotty, T Follicular helper cell biology: a decade of discovery and diseases, Immunity 50 (2019) 1132–1148, https://doi.org/10.1016/j.immuni.2019.04.011.

[52] T. Grune, T. Reinheckel, R. Li, J.A. North, K.J. Davies, Proteasome-dependent turnover of protein disulfide isomerase in oxidatively stressed cells, Arch. Biochem. Biophys. 397 (2002) 407–413, https://doi.org/10.1006/abbi.2001.2719.

[53] A. Kozarova, I. Sliskovic, B. Mutus, S.E. Simon, P.C. Andrews, P.O. Vacratsis, Identification of redox sensitive thiols of protein disulfide isomerase using isotope coded affinity technology and mass spectrometry, J. Am. Soc. Mass Spectrom. 18 (2007) 260–269, https://doi.org/10.1016/j.jasms.2006.09.023.

[54] M. Okumura, K. Noi, S. Kanemura, M. Kinoshita, T. Saio, Y. Inoue, T. Hikima, S. Akiyama, T. Ogura, K. Inaba, Dynamic assembly of protein disulfide isomerase in catalysis of oxidative folding, Nat. Chem. Biol. 15 (2019) 499–509, https://doi.org/10.1038/s41589-019-0268-8.

[55] R. Sgarbanti, L. Nencioni, D. Amatore, P. Coluccio, A. Fraternale, P. Sale, C.L. Mammola, G. Carpino, E. Gaudio, M. Magnani, M.R. Ciriolo, E. Garaci, A.T. Palamara, Redox regulation of the influenza hemagglutinin maturation process: a new cell-mediated strategy for anti-influenza therapy, Antioxid. Redox Signal. 15 (2011) 593–606, https://doi.org/10.1089/ars.2010.3512.

[56] D. Amatore, I. Celestino, S. Brundu, L. Galluzzi, P. Coluccio, P. Checconi, M. Magnani, A.T. Palamara, A. Fraternale, L. Nencioni, Glutathione increase by the n-butanoyl glutathione derivative (GSH-C4) inhibits viral replication and induces a predominant Th1 immune profile in old mice infected with influenza virus, FASEB BioAdvances 1 (2019) 296–305, https://doi.org/10.1096/fba.2018-00066.

[57] D.K. Meyerholz, A.P. Beck, Fundamental concepts for semiquantitative tissue scoring in translational research, ILAR J. 59 (2019) 13–17, https://doi.org/10.1093/ilar/ilaa014.

[58] D. Cortes Selva, A.L. Ready, K.C. Fairfax, Interleukin-4 (IL-4) maintains lymphocyte-stromal cell axis in peripheral lymph nodes, J. Immunol. 198 (2017) 63.19, https://doi.org/10.1002/eji.201847789.

[59] I.S. Junttila, Tuning the cytokine responses: an update on interleukin (IL)-4 and IL-13 receptor complexes, Front. Immunol. 9 (2018) 888, https://doi.org/10.3389/fimmu.2018.00888.

[60] A.H. Lee, N.N. Iwakoshi, K.C. Anderson, L.H. Glimcher, Proteasome inhibitors disrupt the unfolded protein response in myeloma cells, Proc. Natl. Acad. Sci. U. S. A. 100 (2003) 9946–9951, https://doi.org/10.1073/pnas.1334037100.

[61] B.G. Barwick, V.A. Gupta, P.M. Vertino, L.H. Boise, Cell of origin and genetic alterations in the pathogenesis of multiple myeloma, Front. Immunol. 10 (2019) 1121, https://doi.org/10.3389/fimmu.2019.01121.

[62] B. Ribourtout, M. Zandecki, PC morphology in multiple myeloma and related disorders, Morphologie 99 (2015) 38–62, https://doi.org/10.1016/j.morpho.2015.02.001.

[63] S. Granell, G. Baldini, Inclusion bodies and autophagosomes: are ER-derived protective organelles different than classical autophagosomes? Autophagy 4 (2008) 375–377, https://doi.org/10.4161/auto.5605.

[64] K. Asha, N. Sharma-Walia, Virus and tumor microenvironment induced ER stress and unfolded protein response: from complexity to therapeutics, Oncotarget 9 (2018) 31920–31936. doi:10.18632/oncotarget.25886.

[65] R.R. Crawford, E.T. Prescott, C.F. Sylvester, A.N. Higdon, J. Shan, M.S. Kilberg, I.N. Mungrue, Human CHAC1 protein degrades glutathione, and mRNA induction is regulated by the transcription factors ATF4 and ATF3 and a BiPartite ATF/CRE regulatory element, J. Biol. Chem. 290 (2015) 15878–15891, https://doi.org/10.1074/jbc.M114.635144.

[66] A. Fraternale, M.F. Paoletti, A. Casabianca, L. Nencioni, E. Garaci, A.T. Palamara, M. Magnani, GSH and analogs in antiviral therapy, Mol. Asp. Med. 30 (2009) 99–110, https://doi.org/10.1016/j.mam.2008.09.001.